

Effect of different organic amino cations on SAPO-34 for PES/SAPO-34 mixed matrix membranes toward CO₂/CH₄ separation

N. N. R. Ahmad, H. Mukhtar, D. F. Mohshim, R. Nasir, Z. Man

Department of Chemical Engineering, Universiti Teknologi PETRONAS, Perak Darul Ridzuan, Malaysia

Correspondence to: H. Mukhtar (E-mail: hilmi_mukhtar@petronas.com.my)

ABSTRACT: Mixed matrix membranes (MMMs) embedded with functionalized SAPO-34 were successfully synthesized and characterized. Two different types of organic amino cation, namely ethylenediamine (EDA) and hexylamine (HA), were used to functionalize SAPO-34 particles prior to MMM synthesis. In this work, the effects of different functionalizing agents on the membrane morphology, pore size, and CO₂/CH₄ gas separation properties were investigated. Surface modification of SAPO-34 was confirmed via X-ray photoemission spectroscopy (XPS) where the presence of nitrogen atom was observed for the samples functionalized with amino cations. The dispersion of EDA-functionalized SAPO-34 particles was found to have better polymer/filler interface morphology as shown by field emission scanning electron microscopy (FESEM) analysis. The gas separation performance revealed that PES containing EDA-functionalized SAPO-34 exhibited better CO₂/CH₄ separation performance as compared to the MMMs containing HA-functionalized SAPO-34. © 2016 Wiley Periodicals, Inc. *J. Appl. Polym. Sci.* **2016**, *133*, 43387.

KEYWORDS: membranes; morphology; properties and characterization

Received 1 August 2015; accepted 28 December 2015

DOI: 10.1002/app.43387

INTRODUCTION

CO₂/CH₄ gas separation process has drawn a great attention due to its significant development in the industrial applications such as natural gas purification and recovery of CH₄ from landfill gas.^{1,2} For natural gas sweetening, various technologies have been applied for its purification such as absorption, adsorption, cryogenic condensation, and membrane technology.^{3,4} Among these technologies, membrane-based separation has been emerged as an attractive technology due to its simplicity, low capital investment, and high product recovery.⁵ Currently, polymeric-based membranes are commercially available in industrial gas application due to their desirable mechanical properties and economic reliability. However, the separation factor of polymeric membranes is limited as given by Robeson “upper bound” where the permeability is inversely proportional to its selectivity.⁶ This situation leads to the development of mixed matrix membrane (MMM) which combines superior properties of inorganic fillers (i.e., high selectivity and thermally stable). SAPO-34 zeolite is one of the inorganic materials that has been extensively employed in the synthesis of MMM for CO₂ gas separation.^{7–12} The molecular structure of SAPO-34 with pore size around 0.38 nm makes it as a promising filler for CO₂/CH₄ gas separation application since it is larger than CO₂ gas kinetic diameter (0.33 nm) and similar with CH₄ kinetic diameter (0.38 nm).¹³

In order to synthesis a good MMM with excellent gas separation performance, several challenges need to be addressed. The issues include particles agglomeration, non-uniform particles distribution, and poor interaction between polymer and inorganic filler surface.^{14–16} Poor polymer/filler interaction has resulted in the void formation around the fillers which eventually cause the gas selectivity to decrease. Various methods have been applied in order to overcome this problem and improve the MMM with better interface morphology. The most common technique used is the particles surface modification using silane coupling agent.^{1,7,17–19} The addition of silane coupling agents were found to reduce the formation of voids around the filler but yet to completely eliminate them.¹⁷ Another approach was reported to include the ionic liquid into MMM formulation which can act as the wetting agent around the zeolite and thus, improve the polymer/SAPO-34 interaction.²⁰ Rafizah and Ismail²¹ modified carbon molecular sieve (CMS) with poly(vinyl pyrrolidone) K-15 (PVP) by physical deposition method. The interaction between the attached PVP on the fillers surface with polysulfone (PSF) matrix produced MMM with almost voids-free morphology. However, the compatibility aspect between PVP and the selected polymer matrix in the fabrication of MMM should be considered in this modification technique. Low molecular weight additives (LMWA) such as 2-hydroxy 5-methyl-aniline (HMA), *p*-nitroaniline (pNA), 2,4,6-triaminopyrimidine (TAP) can also be used as additive to improve the

polymer/filler interface as reported previously.^{8,22,23} This technique was based on physical interaction through hydrogen bonding between filler–LMWA–polymer matrices.

In a work done by Venna and Carreon,²⁴ the ethylenediamine (EDA) and hexylamine (HA) were grafted onto the surface of SAPO-34 particles through the formation of coordination covalent bond. In their study, they found that the modified surface of SAPO-34 containing amino functional groups was found to enhance the CO₂ separation of the SAPO-34 inorganic membrane. In the present work, flat sheet polyethersulfone (PES)-based MMMs were successfully prepared by incorporating the SAPO-34 zeolite. In order to improve the adhesion between SAPO-34 particles and polyethersulfone, SAPO-34 filler was modified through functionalization technique using two types of organic amino cation namely EDA and HA. The prepared MMMs were characterized in terms of their morphology and physical properties. The effects different functionalizing agents on SAPO-34 toward the CO₂/CH₄ gas separation performance of MMM were investigated. To the best of our knowledge, no works have been reported on the fabrication of MMM containing functionalized SAPO-34 using the mentioned organic amino cations.

EXPERIMENTAL

Materials

Polyethersulfone (Ultrason® E6020P) (PES) flakes was purchased from BASF, Germany. This polymer was selected as polymer matrix due to its commercial availability and has been successfully used in various applications of gas separation.^{17,20,25} The PES flakes were dried in an oven at 120°C for 24 h in order to remove the absorbed moisture prior to the dope solution preparation. The *N*-methyl-pyrrolidone (NMP, obtained from Merck) was used as solvent since it is known as green solvent and it has low evaporation rate and low toxicity. SAPO-34 with particles size around 2–15 μm was purchased from ACS Material and dried at 150°C for 24 h before use in order to remove the trapped moisture. Analytical grade of EDA and HA were purchased from Merck, Germany and used to functionalize the SAPO-34 particles without any purification. The toluene (R&M) and ethanol (99% purity, Hmbg) were used to wash the functionalized SAPO-34.

Modification and Characterization of SAPO-34 Particles

Different organic amino cations were used to modify the raw SAPO-34 particles. The idea was obtained based on the cited literature by Venna and Carreon.²⁴ About 0.15 mmol of EDA was added into a round bottom flask containing 50 mL of toluene. The solution was stirred for 10 min at room temperature. For functionalization purpose, 0.5 g of SAPO-34 filler was added into the solution and refluxed at 105°C for 6 h. The functionalized SAPO-34 particles were filtered and washed with 50 mL of toluene and 100 mL of ethanol. The particles were then dried at 80°C for 12 h under the vacuum condition. The same procedures were repeated for SAPO-34 functionalization using HA of 0.15 mmol.

Both types of functionalized SAPO-34 particles were characterized using X-ray photoemission spectra (XPS) in order to ana-

lyze the presence of amino groups. This analysis was done to quantify the nitrogen composition on the external surface of SAPO-34. The XPS spectra were obtained by using Thermo Scientific (K-Alpha) system. The surface area and pore size of the unmodified and modified SAPO-34 particles were measured respectively based on N₂ adsorption/desorption technique using the Micromeritics ASAP 2020 porosimeter at 77 K. Prior to measurement, the samples were degassed at 473 K for 5 h under vacuum condition.

Synthesis and Characterization of PES Membrane and Mixed Matrix Membrane

The neat PES polymeric membrane was synthesized by using 20 wt % polymers and this is based on the solvent weight. The dried PES flakes were added consecutively into solvent. The polymer–solvent dope solution was stirred for 24 h at room temperature and the solution is ready for casting. For the MMM preparation, 20 wt % of SAPO-34 (based on polymer weight) was added into the NMP solution and stirred for 1 h. The SAPO-34 suspension was “primed” with ~10% of total weighed PES polymer for 2 h. The remaining amount of polymer was gradually added into the mixture and stirred for 24 h. Prior to casting, the MMM solution was degassed for 30 min in order to remove the trapped bubbles. The same method was repeated for the fabrication of MMMs containing functionalized SAPO-34. All types of membranes were casted on a cleaned glass plate by using a casting knife with gap 90 μm. The casted membranes were preliminary dried for 8 h at 90°C under a vacuum condition in order to avoid a sudden heat change on the membrane which might damage the membrane morphology. In order to completely remove the solvent, the temperature were increased to 160°C as per recent cited literature.^{20,25,26}

The synthesized membranes were characterized by using different equipment. Differential scanning calorimetry (DSC) Mettler Toledo was used to investigate the glass transition temperature (*T_g*) of synthesized membranes. The midpoint temperature of the transition region in the second heating cycle was considered as *T_g* value of a sample.¹⁷ The morphology of the synthesized membranes was observed by using FESEM (Zeiss Supra55 VP). For this purpose, the samples were fractured using liquid nitrogen in order to ensure a smooth result prior to scanning.

Gas Permeance Measurement

The performance of fabricated membranes was evaluated by using gas permeation unit. The permeation testing depends on the pressure of feed phase, area of membrane, and also the gas flux on the permeate side. Pure CO₂ and CH₄ were employed as the tested gases at constant pressure of 2 bar. All tests were carried out at room temperature. The flat sheet membranes were cut into a disc shape with a diameter of 5 cm and dried prior to testing to remove the absorbed moisture. The permeation rate was measured by using a bubble flow meter and the permeance results were calculated based on the volumetric flow rate of the gas after reaching the steady-state condition.

In order to maintain the reproducibility of the results, the time for each bubble to transport from one point to another point was measured for about three times for each membrane. The gas permeance results were presented in gas permeation unit

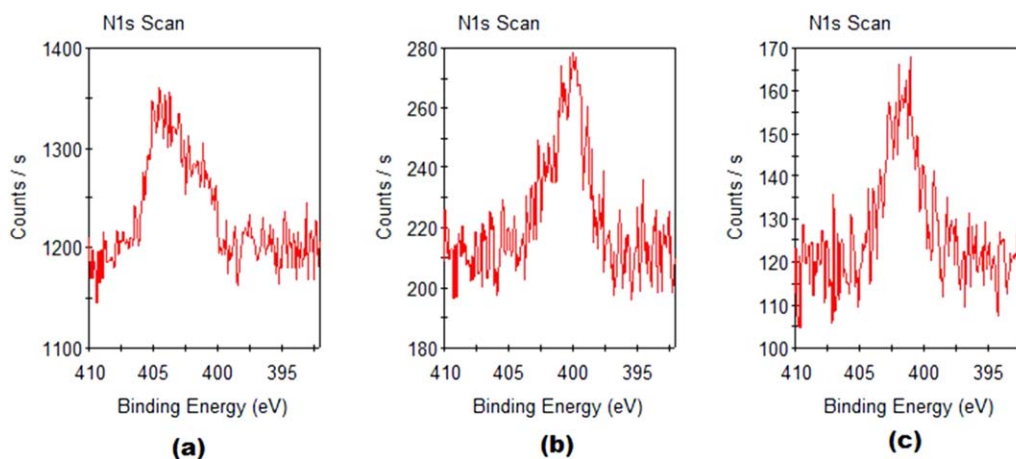


Figure 1. XPS spectra of (a) SAPO-34, (b) SAPO-34-EDA, (c) SAPO-34-HA. [Color figure can be viewed in the online issue, which is available at wileyonlinelibrary.com.]

(GPU) where 1 GPU is equivalent to $10^{-6} \text{ cm}^3 \text{ (STP)} \text{ cm}^{-2} \text{ s}^{-1} \text{ cm Hg}^{-1}$. The following equation [eq. (1)] was used to calculate the gas permeance.

$$\frac{P_i}{L} = \frac{N_i}{\Delta P} \quad (1)$$

The membrane selectivity (α) was calculated by following equation [eq. (2)]:

$$\alpha_{i/j} = \frac{P_i}{P_j} = \frac{\frac{P_i}{L}}{\frac{P_j}{L}} \quad (2)$$

where P_i/L is the gas permeance of component i (GPU), L is the membrane thickness (cm), N_i is the flux of component i ($\text{cm}^3 \text{ cm}^{-2} \text{ s}^{-1}$), ΔP is the pressure difference across the membrane (cm Hg) and $\alpha_{i/j}$ is the ideal gas selectivity of component i over component j .

RESULTS AND DISCUSSION

Characterization of Pure SAPO-34 and Amino-Functionalized SAPO-34

Figure 1 shows the XPS spectra of pure SAPO-34 zeolite and the modified SAPO-34 fillers using different amino cations. From the figure, both EDA and HA-functionalized SAPO-34 showed a peak at the electronic binding energy around 400 eV. This peak could be attributed to the nitrogen atom whose appearance has been previously observed at about 397.2 eV.¹⁷ This finding indicates that the amino groups have been grafted onto the external surface of the SAPO-34. The nitrogen composition on the external surface of SAPO-34 before and after mod-

ification is displayed in Table I. From this table, it can be observed that the pure SAPO-34 particles also have some nitrogen atom trace. The presence of small percentage of the nitrogen atom in the un-modified SAPO-34 particles sample could be attributed to the remaining impurities which were produced during the synthesis process. Furthermore, SAPO-34 functionalized with EDA showed higher N % as compared to the HA-functionalized SAPO-34. This can be explained that EDA consists of two amino groups which can enhance its preferential bonding with the active site on the surface of SAPO-34 particles and consequently increasing the number of grafted amino groups.²⁴

Table II tabulates the surface area and total pore volume of both un-modified and modified SAPO-34, respectively. The results showed a decreasing trend of surface area and total pore volume of modified SAPO-34 as compared to the pure SAPO-34. This has confirmed the amino-grafting on the external surface of SAPO-34. This is consistent with the report from Venna and Carreon²⁴ who observed the similar reduction in surface area. HA-functionalized SAPO-34 exhibited the lower surface area than EDA-functionalized SAPO-34 since HA molecules are bulkier than EDA and consisted of long molecular chain. The decrease of the SAPO-34 surface area as the size of grafting agent getting larger also has been previously observed by other researchers.²⁷ On the other hand, there is no significant change in the total pore volume of SAPO-34-HA as compared to that of SAPO-34-EDA. These results explained that the grafting of HA and EDA molecules mainly took place on the external surface of SAPO-34. Furthermore, it can be suggested that the

Table I. Comparison of Nitrogen Composition on the External Surface of SAPO-34 before and after Functionalization

Filler	Remarks	N %
SAPO-34	Pure SAPO-34 particles	0.72
SAPO-34-EDA	Functionalized SAPO-34 particles	2.58
SAPO-34-HA		2.07

Table II. Comparison of BET Surface Area and Total Pore Volume for Un-modified and Modified SAPO-34

Filler	BET surface area (m^2/g)	Total pore volume (cm^3/g)
SAPO-34	733.38	0.2344
SAPO-34-EDA	614.12	0.1875
SAPO-34-HA	595.39	0.1875

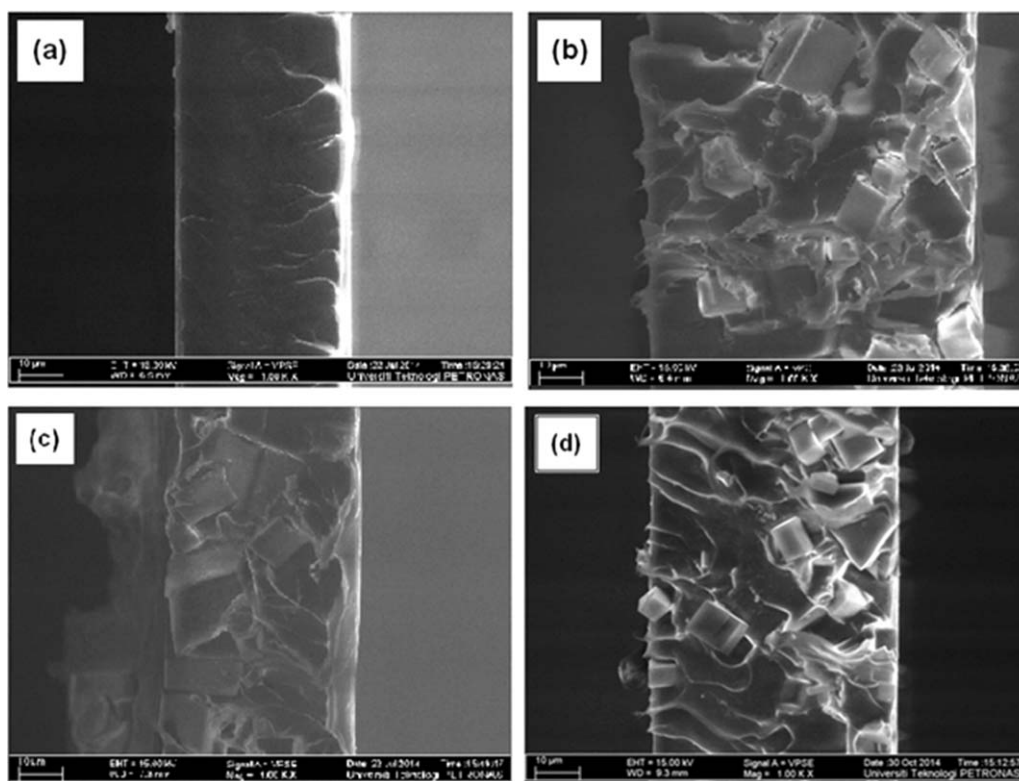


Figure 2. The cross-sectional morphology of (a) PES polymeric membrane, (b) PES/SAPO-34 MMM, (c) PES/SAPO-34-EDA MMM, (d) PES/SAPO-34-HA MMM.

functionalization of these molecules may occur to a large extent at the pore entrance of zeolite.²⁷

Characterization of Pure PES Polymeric Membrane and PES-Based MMM

The cross-sectional morphology for PES pure membrane and MMMs are illustrated in Figure 2. The cross-sectional images of all synthesized membranes showed dense structure. It should be noted that the cubic particles in Figure 2(b–d) are representing the SAPO-34 particles. Figure 2(b) shows that the incorporation of pure SAPO-34 particles into the PES membrane resulted in poor adhesion between the filler and the polymer. This can be observed by the formation of some dark area around the SAPO-34 particles which indicate the voids. On the other hand, the cross-sectional morphology of MMM synthesized with EDA-functionalized SAPO-34 seems to have an improved structure where the polymer/SAPO-34 interface showed a better compatibility. However, the morphology of MMM incorporated with HA-functionalized SAPO-34 did not have much difference as compared to the pure PES/SAPO-34 membranes since there were some voids observed around the filler particles. The EDA-functionalized SAPO-34 particles which contained high content of amino groups (result as confirmed by XPS analysis) have more chances to interact with the polymer chain through hydrogen bonding. This phenomenon had improved the adhesion between the polymer and EDA-modified SAPO-34 particles. On the contrary, the HA-functionalized SAPO-34 did not improve the adhesion between polymer and filler due to less amino presence in HA.

Table III tabulates the effect of amino-functionalized SAPO-34 toward the glass transition temperature of the synthesized MMMs. The T_g value of pure PES polymeric membrane was found to be at 217°C which is comparable with the T_g value reported previously.¹⁷ However, there was a small increase in the T_g value upon the addition of SAPO-34 into the PES membrane. This could be due to the restricted mobility of polymer chain at zeolite interface which was also observed by Li *et al.*¹⁷ However, for PES membrane incorporated with EDA-functionalized SAPO-34, two T_g values were observed where the second T_g was slightly higher than the first one. It was reported that a composite material which consists of two T_g values possibly represent the formation of rigidified region in that material.²⁸ The rigidified region can be formed at the polymer/SAPO-34 interface if the interaction between these two phases is compatible.¹⁶ In the case of EDA-functionalized SAPO-34, a better adhesion between the polymer and SAPO-34 was observed by FESEM images [Figure 2(c)] which support the

Table III. Comparison of Glass Transition Temperature for Different Types of Membranes

Membrane	First T_g (°C)	Second T_g (°C)
PES	217.22	-
PES/SAPO-34	222.25	-
PES/SAPO-34-EDA	220.37	231.18
PES/SAPO-34-HA	223.90	-

findings of these two T_g values. It is suggested that the interaction between the polymer and EDA-functionalized SAPO-34 via the hydrogen bonding restricts the polymer chain mobility. On the other hand, PES membrane with HA-functionalized SAPO-34 exhibited a single T_g value with no significant change as compared to the PES/SAPO-34. Since a less amount of amino molecules groups were grafted for the case of HA-functionalized SAPO-34 (as confirmed by XPS result in Table I), this type of amino-grafting did not much improved the interaction between the polymer and HA-functionalized SAPO-34.

Gas Separation Performance

The results of CO_2 and CH_4 gas permeance are displayed in Figure 3(a, b), respectively, while the CO_2/CH_4 gas selectivity for each membrane is illustrated in Figure 4. Figure 3(a) shows that the addition of SAPO-34 has increased the CO_2 permeance. However, the CO_2/CH_4 selectivity of PES/SAPO-34 membrane did not improve much as compared to that of pure PES membrane. Poor CO_2/CH_4 separation performance is often observed for the case of un-modified zeolite which also reported by previous studies.^{17,29} The increased in gas permeability and the decrease in selectivity could be attributed to the formation of “leaky interface” structure around the particles in MMM which have been proved in earlier discussion through the FESEM analysis.³⁰ The “leaky interface” occurs when the void size is larger than the permeate gas and the resistance at this region is usually lower which attracts the gas molecules to pass through the voids instead of the molecular sieve.³⁰ In addition, the CO_2 gas permeance of PES membrane incorporated with SAPO-34-EDA is lower than that of PES/SAPO-34 membrane. The presence of

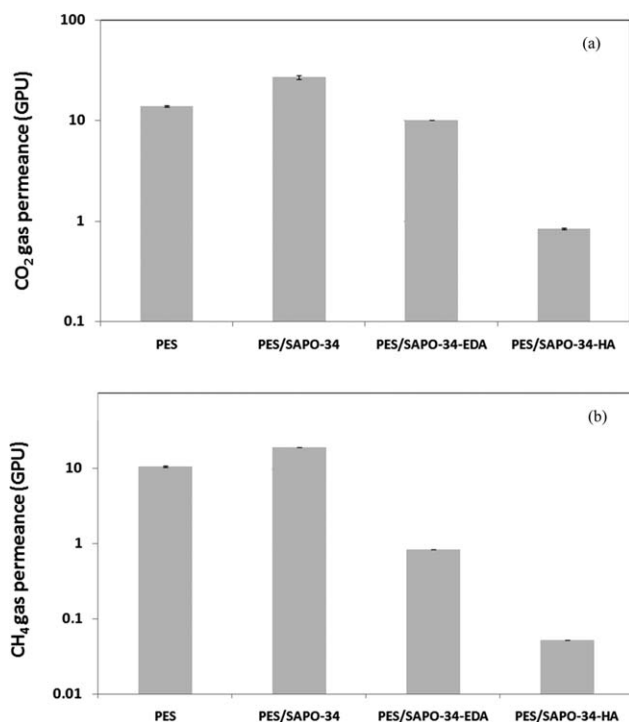


Figure 3. Comparison of (a) CO_2 permeance and (b) CH_4 permeance for all type of membranes.

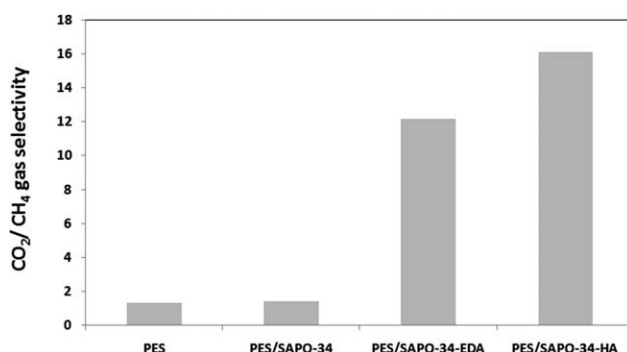


Figure 4. Comparison of CO_2/CH_4 gas selectivity for all type of membranes.

“rigidified region” at the polymer and EDA-functionalized SAPO-34 interface as confirmed by the increase in T_g value (Table III) has possibly enhanced the resistance in gas transport and explained by the decrease of CO_2 permeance. However, the good adhesion between the polymer and EDA-functionalized SAPO-34 has also greatly reduced the permeance of CH_4 molecules which cause the selectivity to increase as compared to the PES/SAPO-34 membrane. For the case of PES/SAPO-34-HA membrane, even though its selectivity is the highest among all membranes, both of CO_2 and CH_4 permeance were observed to reduce significantly which suggests that the pores of zeolite might be blocked with the HA molecules. It is possible for the pore blockage to occur when the bulkier molecules were used to functionalize the zeolite which eventually reduces the gas permeance.²⁴

The gas separation performances of the synthesized MMMs in this work were further compared with the recent works of PES-based MMMs. The comparison is summarized in Table IV. It can be observed that the PES/SAPO34-EDA exhibited a comparable CO_2/CH_4 gas selectivity and significantly having higher CO_2 permeance than the other PES-based MMMs incorporated with montmorillonite clay such as MMT and C15A.^{31,32} The selectivity of the MMMs in this work also improved as compared to the MMMs containing zeolite which has been reported

Table IV. Comparison between the Gas Separation Performance of the Fabricated Membranes in this Work and Selected PES-Based MMMs from Literatures

Membrane	CO_2 gas permeance (GPU)	CO_2/CH_4 selectivity	Reference
PES/SAPO34/20wt %	191.77	15.89	20
PES/MMT/2wt %	0.276	10.2	31
PES/MMT/4wt %	0.165	2.26	31
PES/ TiO_2 /20wt %	0.274	17.3	31
PES/C15/0.75wt %	3.400	18.12	32
PES/Zeo 4A/10wt %	63.96	3.19	33
PES/Zeo 4A/20wt %	24.97	3.20	33
PES/SAPO34-EDA	10.091	12.14	This work
PES/SAPO34-HA	0.835	16.09	This work

by Ahmad *et al.*³³ However, the PES/SAPO34-EDA possessed relatively low CO₂ gas permeance as compared to PES/Zeolite 4A MMM. The distinction can be explained by the fact that their PES membrane consisted of asymmetrical structure.

CONCLUSION

Polyethersulfone MMMs incorporated with non-functionalized and amino-functionalized SAPO-34 zeolite were successfully fabricated in this study. The effects of different types of organic amino cation grafting using EDA and HA on the properties of MMM were analyzed. From the results obtained in this work, it can be concluded that:

- i. The modification of SAPO-34 zeolite using EDA has resulted in higher amino groups grafting as compared to that of HA-grafting based on the XPS analysis report. BET analysis demonstrates that most of the amino groups have been grafted on the external surface of SAPO-34 since the surface area decreased after chemical modification while the pore volume did not have much difference.
- ii. The functionalization of SAPO-34 using organic amino cation has resulted in better polymer/filler adhesion as seen through the cross-sectional morphology analysis by FESEM. The MMM incorporated with EDA-functionalized SAPO-34 showed a good compatibility at the polymer/filler interface which in turn enhanced the CO₂/CH₄ gas separation performance for this type of membrane.
- iii. HA-functionalized SAPO-34 did not significantly improved the physical and thermal properties of modified MMM which leads to poor gas separation performance.

ACKNOWLEDGMENTS

Universiti Teknologi PETRONAS and Ministry of Education (MOE), Malaysia is fully acknowledged for funding this project through Exploratory Research Grant Scheme (ERGS 0153AB-I23).

REFERENCES

1. Ismail, A. F.; Kusworo, T. D.; Mustafa, A. *J. Membr. Sci.* **2008**, *319*, 306.
2. Nasir, R.; Mukhtar, H.; Man, Z.; Mohshim, D. F. *Chem. Eng. Technol.* **2013**, *36*, 717.
3. Shimekit, B.; Mukhtar, H. In *Advances in Natural Gas Technology*; Hamid, A. M. Ed.; InTech: China, **2012**, 235.
4. Mohshim, D. F.; Mukhtar, H.; Man, Z.; Nasir, R. *J. Eng.* **2013**, *2013*, 1.
5. Mannan, H. A.; Mukhtar, H.; Murugesan, T.; Nasir, R.; Mohshim, D. F.; Mushtaq, A. *Chem. Eng. Technol.* **2013**, *36*, 1838.
6. Robeson, L. M. *J. Membr. Sci.* **2008**, *320*, 390.
7. Junaidi, M. U. M.; Khoo, C. P.; Leo, C. P.; Ahmad, A. L. *Micropor. Mesopor. Mater.* **2014**, *192*, 52.
8. Cakal, U.; Yilmaz, L.; Kalipcilar, H. *J. Membr. Sci.* **2012**, *417–418*, 45.
9. Hudiono, Y. C.; Carlisle, T. K.; LaFrate, A. L.; Gin, D. L.; Noble, R. D. *J. Membr. Sci.* **2011**, *370*, 141.
10. Karatay, E.; Kalipcilar, H.; Yilmaz, L. *J. Membr. Sci.* **2010**, *364*, 75.
11. Peydayesh, M.; Asarehpour, S.; Mohammadi, T.; Bakhtiari, O. *Chem. Eng. Res. Design* **2013**, *91*, 1335.
12. Zhao, D.; Ren, J.; Li, H.; Hua, K.; Deng, M. *J. Energ. Chem.* **2014**, *23*, 227.
13. Yeo, Z. Y.; Chew, T. L.; Zhu, P. W.; Mohamed, A. R.; Chai, S. P. *J. Natural Gas Chem.* **2012**, *21*, 282.
14. Süer, M. G.; Baç, N.; Yilmaz, L. *J. Membr. Sci.* **1994**, *91*, 77.
15. Mahajan, R.; Burns, R.; Schaeffer, M.; Koros, W. J. *J. Appl. Polym. Sci.* **2002**, *86*, 881.
16. Aroon, M. A.; Ismail, A. F.; Matsuura, T.; Montazer-Rahmati, M. M. *Sep. Purif. Technol.* **2010**, *75*, 229.
17. Li, Y.; Guan, H. M.; Chung, T. S.; Kulprathipanja, S. *J. Membr. Sci.* **2006**, *275*, 17.
18. Pechar, T. W.; Kim, S.; Vaughan, B.; Marand, E.; Tsapatsis, M.; Jeong, H. K.; Cornelius, C. J. *J. Membr. Sci.* **2006**, *277*, 195.
19. Chen, X. Y.; Nik, O. G.; Rodrigue, D.; Kaliaguine, S. *Polymer* **2012**, *53*, 3269.
20. Mohshim, D. F.; Mukhtar, H.; Man, Z. *Sep. Purif. Technol.* **2014**, *135*, 252.
21. Rafizah, W.; Ismail, A. *J. Membr. Sci.* **2008**, *307*, 53.
22. Şen, D.; Kalipcilar, H.; Yilmaz, L. *J. Membr. Sci.* **2007**, *303*, 194.
23. Yong, H. H.; Park, H. C.; Kang, Y. S.; Won, J.; Kim, W. N. *J. Membr. Sci.* **2001**, *188*, 151.
24. Venna, S. R.; Carreon, M. A. *Langmuir* **2011**, *27*, 2888.
25. Nasir, R.; Mukhtar, H.; Man, Z.; Dutta, B. K.; Shaharun, M. S.; Bakar, M. Z. A. *J. Membr. Sci.* **2015**, *483*, 84.
26. Nasir, R.; Mukhtar, H.; Man, Z.; Shaharun, M. S.; Bakar, M. Z. *RSC Adv.* **2015**, *5*, 60814.
27. Nik, O. G.; Nohair, B.; Kaliaguine, S. *Micropor. Mesopor. Mater.* **2011**, *143*, 221.
28. Moore, T. T.; Koros, W. J. *J. Mol. Struct.* **2005**, *739*, 87.
29. Nik, O. G.; Chen, X. Y.; Kaliaguine, S. *J. Membr. Sci.* **2011**, *379*, 468.
30. Rezakazemi, M.; Ebadi Amooghin, A.; Montazer-Rahmati, M. M.; Ismail, A. F.; Matsuura, T. *Prog. Polym. Sci.* **2014**, *39*, 817.
31. Liang, C. Y.; Uchytil, P.; Petrychkovych, R.; Lai, Y. C.; Friess, K.; Sipek, M.; Mohan Reddy, M.; Suen, S. Y. *Sep. Purif. Technol.* **2012**, *92*, 57.
32. Ismail, N. M.; Ismail, A. F.; Mustafa, A. *Procedia CIRP* **2015**, *26*, 461.
33. Ahmad, S. H.; Othman, M. H. D.; Rahman, M. A.; Jaafar, J.; Ismail, A. *J. Teknol.* **2014**, *69*, 67.